3ème conférence Internationale des énergies renouvelables CIER - 2015
Proceedings of Engineering and Technology – PET
pp.228-236

Heat and Mass Transfer of the μ-PD Process compared to the Cz technique for Ti^{+3}: Al_2O_3 Fiber Crystal Growth.

Hanane Azoui [1], Abdellah.Laidoune[2], Djamel.Haddad[3] and Derradji.Bahloul[4]

[1,2,4]*Département de Physique, Faculté des Sciences de la Matière, Université de Batna 1.*

1Rue Chahid Boukhlouf Mohamed El-Hadi, 05000 Batna, Algeria.

[3]*Département de mécanique, Faculté de l'engineering, Laboratoire (LESEI), , Université de Batna2, Algeria.*

Corresponding Author: Hanane Azoui, anhanane@gmail.com

***Abstract*— In this study, we established a numerical two-dimensional finite volume model, in cylindrical coordinates with an axisymmetric configuration, to find the optimal conditions to grow high-quality crystals. We focus on a comparative study of the heat and masse transfer in the growth of Ti+3: Al2O3between two growing techniques, say the micro-pulling down and Czochralski growth techniques.The melt flow, the heat and mass transfer as well as the interface shapes are modelled by the differential equations of conservation of mass, of momentum, energy and species. Simulations results show that the longitudinal of titanium remains homogeneous along the axis of the sapphire crystal; the radial mass transfer of titanium increase in the crystal drawn when the pulling rate increases. Our model for the μ-PD method is in good agreement with experimental results. Whereas for Czochralski method the experimental results show that, there is a concentration gradient along the pulling axes, i.e. the segregation problem of the dopants towards the periphery, this result leads to a poor optical quality crystals.The melt/crystal interface for the μ-PD technique has a flat shape; this important result from this technique agrees with the experiment observation; whereas the melt/crystal interface in the Cz technique has a convex shape towards the melt, this shape causing the dopants' segregation problem. The numerical simulation results show a good agreement with the experiment data. The developed model provides important information to improve the growth process of titanium doped sapphire and we find that the μ-PD technique give better optical quality crystals compared to Cz method.**

***Keywords*— Heat transfer; Mass transfer; Sapphire; Titanium; Micro-pulling down technique; Czochralski technique.**

I. INTRODUCTION

In the development of techniques, to control the crystal shape in the various methods of growth from the melt, it has been long recognized that the heat and mass transfer in the system growth plays an important role in determining the shape and the quality of the growing crystal [1]. In this work we have studied the heat and the mass transfer in the growth of crystalline fibers of titanium doped sapphire drawn by the micro-pulling down growing technique compared to the Czochralski technique; this study allows us to know the effect of size and geometry of growth system and the pulling rate on the quality crystals exactly for the development of laser systems. We chose the sapphire because is a very important material because of its exceptional chemical and physical properties [2]. For this raison sapphire is used widely in a number of modern high-tech applications, say several military, environmental, medical, and industrial applications [3, 4]. When titanium doped sapphire, this material has excellent mechanical, thermal, and optical properties which allow the development of various systems especially laser systems [5]. Many growing techniques have been used to grow this material (titanium doped sapphire) such as Czochralski (CZ) [6, 7], Heat exchanger method (HEM) [8] Kyroupolos (KY) [9] and pulsed laser deposition (PLD) [10, 11]. More recently there has been intense interest in using the micro-pulling-down method for the growth of shaped crystals fibers in a wide variety of domains, especially for laser, medical and optics application [12]. There are not a lot of numerical studies performed investigating these heat and mass transfer during the growth process of this material using the μ-PD or Cz technique. Our aim is to perform a comparative study between tow these techniques. In [13] a global modelling is performed by H.S. Fang et al to predict electromagnetic field, heat transfer,

melt flow, and thermal stress during RF-heated Czochralski (Cz) single crystal growth of sapphire. They also Chung-Wei Lu et al [14] found that although the maximum values of temperature and velocity decrease, the least input power is required if the central position of the RF coil is maintained below the central position of the melt during the crystal growth process, the convexity of the crystal–melt interface increases as the crystal length grows. For the μ-PD method, A. Nehari et al established a simple monodimensional analytical model for study the axial chemical segregation in micro-PD, the results obtained are supported by experiments of Ti^{+3}: Al_2O_3 fiber pulling by the μ-PD method [15]. They also H. S. Fang et al studied numerically the steady-state heat transfer, fluid flow, and interface shape in a μ-PD process for Al2O3 fiber crystal; they found that, in the melt, Marangoni convection is dominant, and the buoyancy convection is negligible Gas convection is strong, heat transfer around the crucible region is dominated by radiation [16]. In this work a numerical model is established for Ti^{+3}: Al_2O_3 crystal growth process to find the optimal conditions to grow high-quality crystals; in a comparative study between two growing techniques, the micro-pulling down and Czochralski. We focus on the heat and the mass transfer, interface shapes, streamlines, as well as on the thermal filed. The study of the problem is simplified to an incompressible and Newtonian flow of a viscous molten Ti^{+3}: Al_2O_3 that is governed by the Navier-Stokes, heat and mass transfer equations under the Boussinesqapproximation, while the flow is laminar.

The next section summarizes the mathematical formulation of our model that is the governing equations, the boundary conditions and the numerical scheme used in our simulations. Section 3 is devoted to the results and discussion, followed by conclusions in section 4. Model and solution scheme

The system to be modeled is sketched in Fig.1.

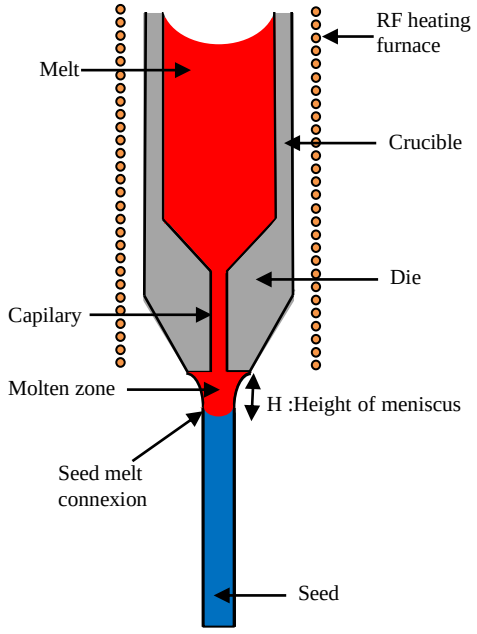

Fig.1 Schematic diagram of domain of μ-PD.

The raw material (red color) is put in the crucible and heated until melting by using RF (Radio frequency) heating furnace. The μ-PD technique uses a capillary die for the growth of shaped crystals [2]. The growth is generated by the connection of the seed (blue color) with the drop at the bottom of the capillary die in the crucible.

In Fig.2 we present the radio frequency (RF) μ-PD machine, which consists of a crucible, a generator operates and frequency units [12].

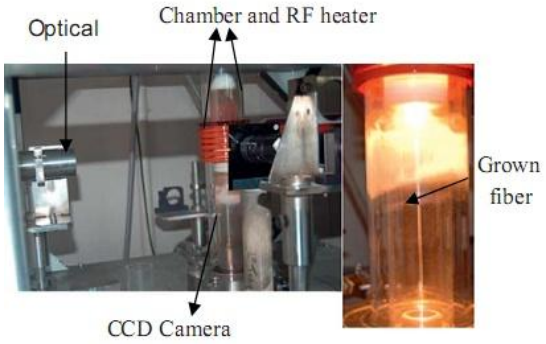

Fig.2 Apparatus of the μ-PD machine growth [11].

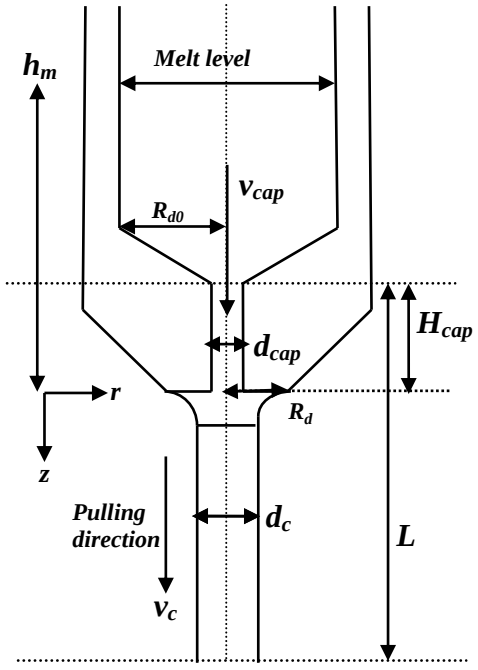

Fig. 3 Schematic diagram of the computational domain

This apparatus allows the growth of crystal with stable diameters, where the visualisation of the grown crystal is controlled by CCD camera. A computational domain of the micro-pulling down is illustrated in Fig.3. WhereR_{d0} is the inner radius of crucible, R_d is the crucible radius at the bottom, R_c=d_c/2is the radius of the crystal; while dc and dcap are the diameters of the growing crystal and the capillary respectively (fig.3).

A. Governing Equations

Dimensionless variables are defined by scaling lengths by Rd , velocity by α_m/R_d , temperature by the melting point T_m , and concentration by C_0, where α_m is the thermal diffusivity of the melt [17]. We have used a two dimensional axisymmetric model because of the cylindrical symmetry of the problem. The equations governing the dynamics of the melt flow resulted from the principles of conservation of mass, momentum and energy in the melt and in the crystal. The flow, the heat and the mass transfer are modelled by the dimensionless differential equations:

Equation of radial component of the momentum:

$$\frac{\partial u}{\partial t}+u\frac{\partial u}{\partial r}+v\frac{\partial u}{\partial z}=-\frac{\partial P}{\partial r}+$$
$$\Pr\left(\frac{\partial}{\partial r}\left(\frac{1}{r}\frac{\partial}{\partial r}\left(r.u\right)\right)+\frac{\partial}{\partial z}\left(\frac{\partial u}{\partial z}\right)\right) \quad (1)$$

Equation of axial component of the momentum:

$$\frac{\partial v}{\partial t}+u\frac{\partial v}{\partial r}+v\frac{\partial v}{\partial z}=-\frac{\partial P}{\partial z}+\Pr.\frac{\partial}{\partial r}\left(\frac{1}{r}\frac{\partial}{\partial r}\left(r.v\right)\right)+$$
$$\Pr.\frac{\partial}{\partial z}\left(\frac{\partial v}{\partial z}\right)-\Pr.Ra_T.T+\frac{\Pr^2}{Sc}.Ra_S.C \quad (2)$$

Conservation equation:

$$\nabla.V=\frac{1}{r}\frac{\partial\left(r.u\right)}{\partial r}+\frac{\partial v}{\partial z}=0 \quad (3)$$

Energy equation:

$$r\frac{\partial T}{\partial t}+\frac{\partial}{\partial r}\left(r.u.T\right)+\frac{\partial}{\partial z}\left(r.v.T\right)=$$
$$\frac{\partial}{\partial r}\left(r.\alpha_i\left(T\right)\frac{\partial T}{\partial r}\right)+\frac{\partial}{\partial z}\left(r.\alpha_i\left(T\right)\frac{\partial T}{\partial z}\right) \quad (4)$$

Dopant concentration equation:

$$r\frac{\partial C}{\partial t}+\frac{\partial}{\partial r}\left(r.u.C\right)+\frac{\partial}{\partial z}\left(r.v.C\right)=$$
$$\frac{\Pr}{Sc}.\left(\frac{\partial}{\partial r}\left(r.\frac{\partial C}{\partial r}\right)+\frac{\partial}{\partial z}\left(r.\frac{\partial C}{\partial z}\right)\right) \quad (5)$$

Where Pr is the Prandtl number ($\Pr=\alpha_m/\nu_m$, where ν_m is the kinematic melt viscosity), *Sc* is the Schmidt number ($Sc=\nu_m/D$, and *D* the diffusivity of titanium in the melt). Also α_i is the thermal diffusivity of phase *i*, *i=c* for crystal and *i=m* for melt. Ra_T, Ra_S : the thermal and solutal Rayleigh number respectively, are two important dimensionless variables in the source term of the equation of momentum they are defined as follows [17]:

$$Ra_T=\frac{g\beta_T T_m R_d^{\,3}}{\alpha_m\nu_m};\ Ra_S=\frac{g\beta_S C_0 R_d^{\,3}}{\alpha_m\nu_m}$$

The thermal and solutal expansion coefficients are β_T and β_S respectively, and g is the gravitational acceleration. The governing equations with their associated boundary conditions are discretized by a finite volume method (*FVM*). Boundary conditions are also required to solve the above governing equations.

II. BOUNDARY CONDITIONS

It is assumed that the solute is uniformly distributed in the melt reservoir and its concentration is C_0. The solute diffusion in the solid phase is neglected. These governing equations with their associated boundary conditions are discretized by a finite volume method (FVM). We present below a detailed description about the boundary conditions used in our simulations that are the same in reference [17]. Some important boundary conditions are described here.

A. Boundary conditions at the symmetric axis

In our two dimensional axisymmetric model, the boundary condition at the symmetric axis for the physical quantities is set as follows:

$$\frac{\partial\phi}{\partial r}=0$$

In the above equations, ϕ is the physical propriety (velocities (*u*,*v*), temperature *T*, and concentration *C*).

The boundary conditions for heat and mass transfer are set as follows:

B. Temperature boundary conditions

At the top entrance the temperature is set by the radio frequency generator it's about $\Delta T\approx$20 to 30 Kelvin above the melting point of sapphire:

$$T=T_m+\Delta T$$

At the liquid-solid interface the boundary condition is:

$$\rho_C \Delta H v_C + K_m \vec{\nabla} T_m . \vec{n} = K_C \vec{\nabla} T_C . \vec{n}$$

ΔH is the latent heat of sapphire, v_C is the growth velocity , ρ_C the crystal density; and K_C the thermal conductivity of crystal.

At the surface of the material, heat transfer from the system to the ambient is by convection according to the energy balance along the material surface:

$$\vec{n}.K_i \vec{\Delta} T = -Bi\left(T - T_a\right)$$

Where $\vec{n}$ is the unit normal vector on the melt or crystal surface pointing outwards; K_i is the ratio of thermal conductivity of phase i to the melt; where (i=*m(melt)*, i=*c(crystal)*) and $Bi = hR_d / K_m$ is the Biot number.

In this study the ambient temperature T_a is set to be a constant.

- At the end of the fiber $z = L$ using the fixed-temperature boundary condition, i.e. $T = T_a$.

C. Solute concentration boundary conditions

- At the top entrance $\left(z = -H_{cap}\right)$, the solute boundary condition is given by the solute flux balance:

$$\vec{e}_z . \vec{\nabla} C = \left(\frac{Sc}{\Pr}\right) Pe_m \left(C - 1\right)$$

Where $\vec{e}_z$ is the unit vector along the z axis, and $\vec{\nabla} C$ is the gradient of the concentration.

- The Neumann condition is imposed at the melt/crystal interfaces:

$$\vec{n}.\vec{\nabla} C = \left[\left(\frac{\rho_C}{\rho_m}\right) - K\right]\left(\frac{Sc}{\Pr}\right) Pe_c \, C\left(n.e_z\right)$$

Where K is the segregation coefficient according to the phase diagram, and $\vec{n}$ is the unit normal vector at the growth front pointing to the melt.

$Pe_m = v_m R_d / \alpha_m$, $Pe_c = v_C R_d / \alpha_m$ are the Peclect numbers of the melt and crystal respectively.

D. Velocity boundary conditions

The radial and axial velocities at the top entrance given by:

$$u = u_0 = 0$$

$$v = v_{cap} = \left(\frac{\rho_C}{\rho_m}\right)\left(\frac{d_C}{d_{cap}}\right)^2 v_C$$

Where v_C is the growth velocity, and v_{cap} is the flow velocity in capillary channel as showing in Fig.3.

At the wall inside the capillary,

$$u = 0 \; ; \; v = 0$$

In the free surface, the two components of the velocity are deduced from Marangoni convection; where the tangential stress balance is required:

$$ns : t = Ma\left(s.\nabla T\right)$$

Where s is the unit tangent vector at the free surface, Ma is the Marangoni number and t the shear stress tensor. In the crystal, velocity boundary condition is:

$$v = v_C$$

III. Results and Discussion

In the present study, we are interested only in cases where Titaniumconcentration is 0.1% in the melt (Al_2O_3) which was used in the previous experiments [18]. The physical properties of Ti^{3+}, Al_2O_3 used in calculations are listed in Table I [16, 18, 19, 20].

TABLE I
PHYSICAL PROPERTIES OF Ti^{3+}: AL_2O_3

Physical Properties
Cp_c = 1300 (J/Kg. K)
Cp_m = 765 (J/Kg. K)
K_c = 17.5 (W/m.K)
K_m = 3.5 (W/m.K)
μ_m = 0.0475 (Kg/m.s)
T_m=2323 K
β_T =0.0475 K^{-1}
ΔH=1.8×10^{-5} (J/Kg)
K=1
ρ_c=3960 (Kg/m^3)
ρ_m=3500 (Kg/m^3)
Φ_0=17^0

A. Masse transfer (distribution) of the titanium in the sapphire material

1) Axial mass transfer in µ-PD process

The distribution of the dopants concentration of titanium along the axis of the crystal of titanium-doped sapphire (solid) for various pulling rate is illustrated in the Fig4. (0.3, 0.5, 0.8 and 1(mm/min)) are the pulling rates used in our simulation, that are the same in the experimental work [18].

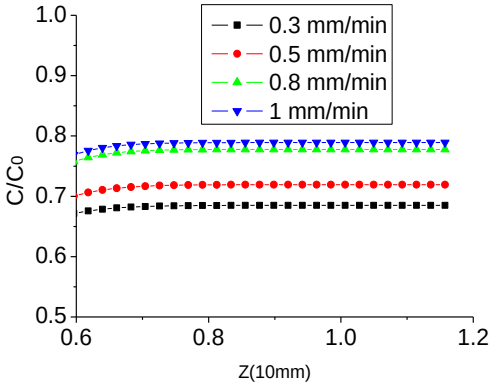

Figure.4: Results of our simulation.

In the figure.4 as the fluid particles go downwards (z>0.6 : the fiber), we notice that the longitudinal distribution of the Ti^{3+} remains homogeneous along the axis of the fiber [18], even for relatively high pulling rates compared to other growth techniques as Czochralski. These results is in good agreement with experimental results shown in the Figure5 [18], and give a good optical and thermal quality of crystal for various applications, especially for optoelectronics and laser applications.

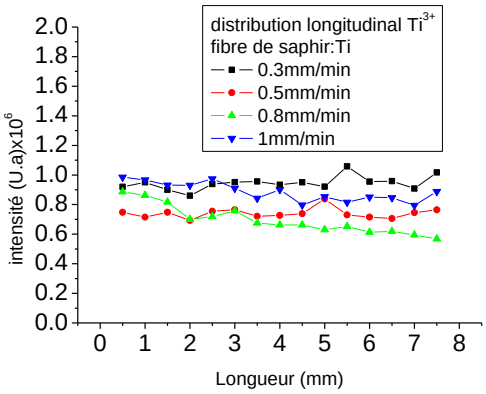

Fig.5 Results of experimental [18].

2) Radial mass transfer in the µ-PD system

Fig. 6 illustrates the radial distribution in the center (r=0 µm) and in the periphery ($r=0.3\times10^3$µm) of the fiber of sapphire. We notice the increasing of Ti^{+3} radial concentrations with the increasing of the pulling rate in the case of our simulation.

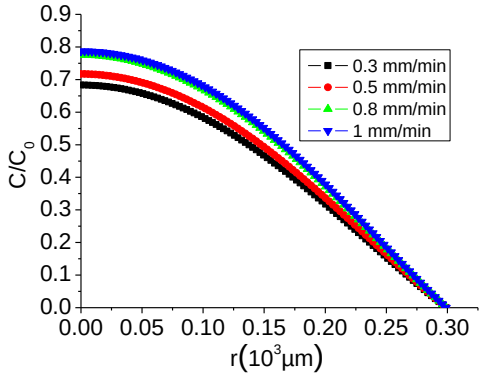

Fig.6 Dopants radial distribution.

This result agrees again with the experimental results for the three pulling rate: 0.5, 0.8 and 1(mm/min) shown at the Fig 7. We add another result that regards by the distribution of Ti^{+3} in the periphery ($r=0.3\times10^3$µm) where this distribution almost zero and this is avoids the problem of segregation.

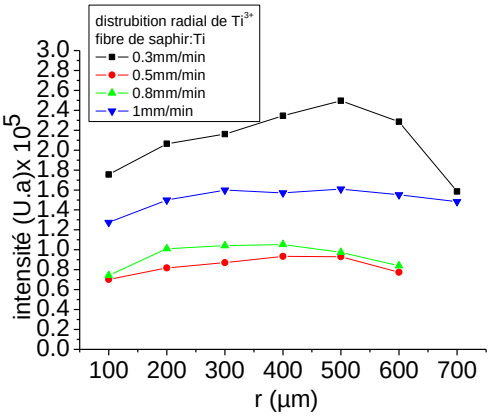

Fig.7 Radial distribution. Experimental [2].

We also notice an increase of Ti^{+3}radial concentrations with the pulling rate in the case of our simulation and this is one of the advantages of the µ-PD method over the CZ technique which induces the segregation of the dopants towards the periphery as showing in the figure below.

3) Study of Ti^{3+} segregation versus the pulling rate

In order to study the mass transfer of titanium versus the pulling rate of different parts in the fiber, the following curve was plotted, We notice that titanium concentration increases with the pulling rate. This result was verified in the three parts of fiber.

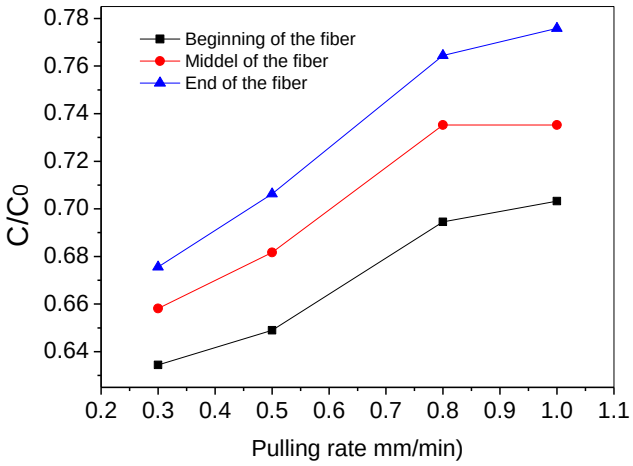

Fig .8 The concentration of dopants of three parts in the fiber versus the different pulling rate.

4) Radial mass transfer in Czochralski (Cz) technique

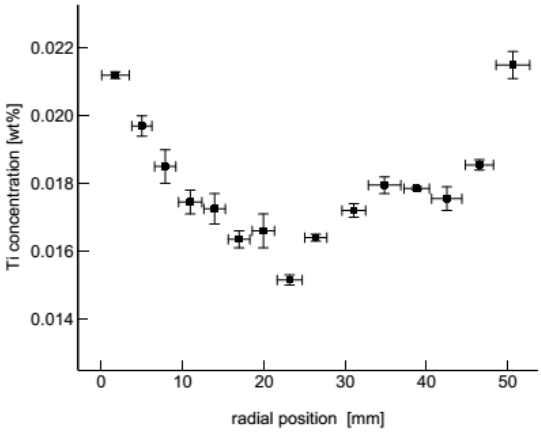

Figure.9. Dopants radial distribution of Ti along the diameter of sapphire crystal [7].

For the growth of Ti^{+3}:Al_2O_3 crystals Al_2O_3 by this technique; the starting material (melting point T_m= 2323 K) with small additives of typically 1 % of titanium which was used in our simulation and in the previous experiments [18]. Figure.9 illustrates the Ti dopants radial distribution in the Czochralski process; we notice that there is a concentration gradient along the pulling axes, i.e. the segregation problem of the dopants towards the periphery [7], whereas for the micro pulling down (µ-PD) technique the high pulling rate and the geometry helps the gathering of dopants in the center of the crystal not towards the periphery [18, 19].

B. Effect of the geometry of the µ-PD technique compared to the Cz geometry

For the Czochralski (Cz) technique: We notice that the liquid is subjected to circulate in a large eddy driven by natural convection and Marangoni convection on the free surface. Fig.10.b shows the flow of fluid particles near the walls and near the free surface, where the dopants outwards to the periphery (red color) causing the dopants' segregation problem which represent a shortcoming of this technique.

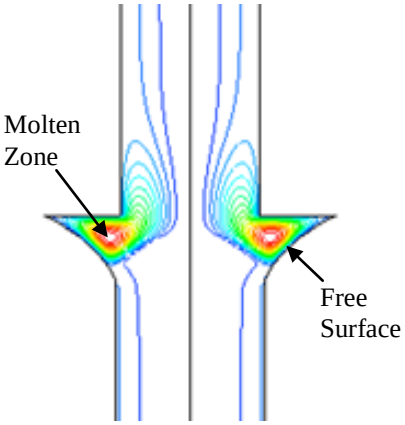

Fig.10 .a: Representation of the Streamline in the micro-pulling-down process (mm).

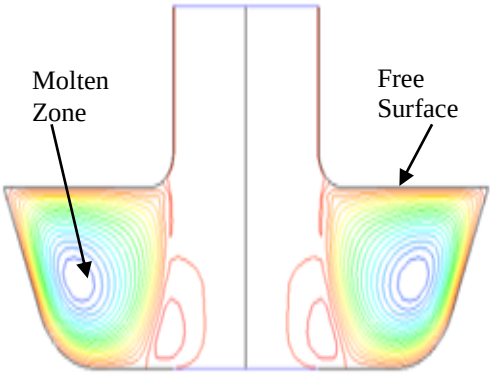

Fig10.b: Representation of the streamline in the Czochralski process (cm).

Whereas, the micro pulling down geometry helps to avoid the dopants' segregation problem as shown in Figure.10.a and this is one of the advantages of this method over other growing methods. In fact, there is no such flow near the free surface (blue color). This due to the small dimensions (mm, µm) involved in the micro pulling technique. So the geometry

of the micro-pulling down avoids the segregation problem of the dopants towards the periphery.

C. *Heat transfer in the growth system of µ-PD and Czochralski techniques*

The quality of the crystals is governed by many factors, citing the dynamics of drawing, mass and heat transfer, effect of convection, the geometry of the melt/crystal interface. The shape of melt/crystal interface plays an important role for the quality of the material drawn. The shape of this interface is essentially determined by the heat transfer in the growing system [14]. Figure 11 shows the heat transfer (Temperature contour plot) in the micro pulling down and Czochralski system, such as blue color shows the solid or Ti^{+3}:Al_2O_3 crystal and red color shows the fluid or the melt. According to these results the melt/crystal interface for the µ-PD techniques (Fig.11.a) has a flat shape towards the crystal. This important result from the flat shape of the melt-crystal interface agrees with the experiment observation [18, 19]; whereas the melt/crystal interface in the Czochralski technique has a convex shape towards the melt (Fig.11.b), this convex shape leads to a radial profile of the Ti concentration, this shape causing the dopants' segregation problem [7].

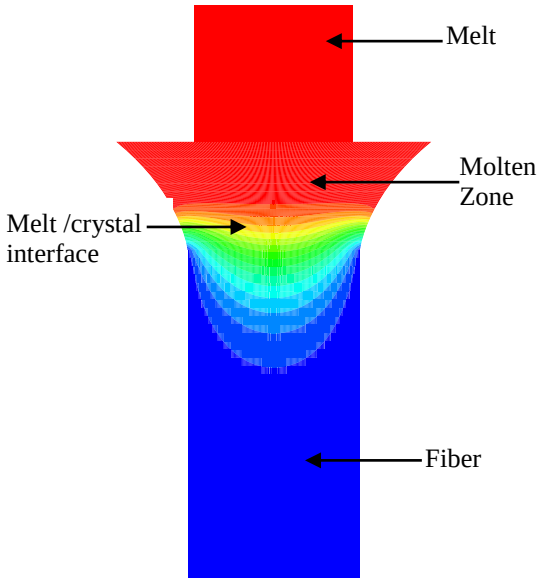

Fig.11.a. Heat transfer showing in the growth system of: µ-PD .

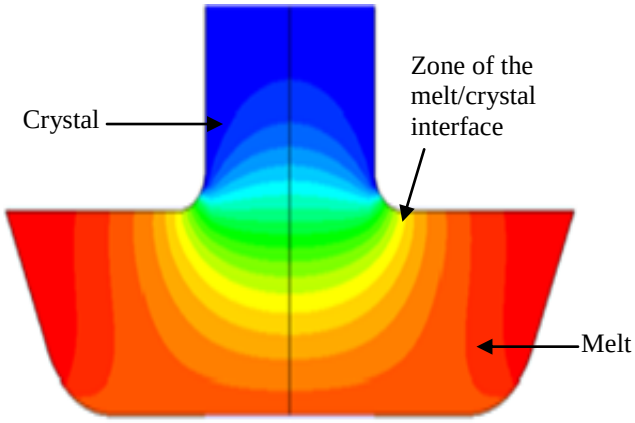

Fig.11.b. Heat transfer showing the melt/crystal interface in the growth system of: µ-PD and Czochralski .

IV. Conclusions

We have developed a numerical model to analyze the micro-pulling-down growth of Ti^{+3}: Al_2O_3 fibers compared to the Czochralski (Cz) technique for the laser application. The heat and mass transfer, melt flow, interface shapes, streamlines, as well as the thermal filed, are computed simultaneously using the Finite Volumes Method (FVM); We conclude that:

-The longitudinal mass transfer (distribution of the Ti^{3+}) remains homogeneous along the axis of the sapphire fiber even for relatively high pulling rates. Our results are in good agreement with experimental results, and this homogeneity gives a material with a good optical and thermal quality for several applications.

-The radial mass transfer of titanium increase in the crystal drawn when the pulling rate increases.

-The heat transfer gives information on the shape of the melt/crystal interface; which plays an important role for the optical and thermal quality of the material drawn.

-The geometry of the µ-PD avoids the segregation problem of the dopants towards the periphery, and pulling rate helps the gathering of dopants in the center of the crystal. whereas we notice for the Cz method that there is a concentration gradient along the pulling axes, i.e. the segregation problem.

-The heat transfer in the growing system determines the shape of the melt-crystal interface; the shape of this interface for the µ-PD method agrees with the experiment observation and it essentially plays an important role for the quality of the crystal drawn.

-Therefore, for the micro pulling down (µ-PD) method, the results obtained are important for laser applications. Indeed, for other growth methods such as Cz, it is not easy to avoid the problem of segregation to the periphery, whereas the µ-PD promotes the gathering of impurities towards the axis of the fiber making a good overlap with the laser beam when the fiber is used as amplifying medium in a laser.

ACKNOWLEDGMENT

The author is grateful for the support of the Prof Lebbou Kheirreddine (Directeur de recherche CNRS Institut Lumiere Matiere); University of Lyon1-France.

REFERENCES

[1] Wencheng Ma, Lili Zhao, Guoqiang Ding, Yang Yang, Tiezheng Lv, Ming Wu, Lijun Liu. Numerical study of heat transfer during sapphire crystal growth by heatexchanger method. International Journal of Heat and Mass Transfer 72 (2014) 452–460.

[2] Fukuda T., Shaped Crystals, Growth by Micro- Pulling- Down Technique .Advances IN materials Research 8, 2007.

[3] THIERRY DUFFAR. Crystal Growth Processes Based on Capillarity. Czochralski, Floating Zone, Shaping and Crucible Techniques. © 2010 John Wiley & Sons Ltd.Y.

[4] Chandra P. Khattak, Frederick Schmid, Growth of the world's largest sapphire crystals, Journal of Crystal Growth. 225 (2001).

[5] G. Alombert-Goget, K. Lebbou, N. Barthalay, H. Legal, G. Chériaux. Large Ti-doped sapphire bulk crystal for high power laser applications. Optical Materials 36 (2014) 2004–2006.

[6] H. Li, E.A. Ghezal, G. Alombert-Goget, G. Breton, J.M. Ingargiola, A. Brenier, K. Lebbou. Qualitative and quantitative bubbles defects analysis in undoped and Ti-doped sapphire crystals grown by Czochralskitechnique. Optical Materials 37 (2014) 132–138.

[7] Reinhard Uecker ; DetlefKlimm ; Steffen Ganschow ; Peter Reiche ; Rainer Bertram ; Mathias Roßberg ; Roberto Fornari. Czochralski growth of Ti:sapphire laser crystals. Proc. SPIE 5990, OpticallyBased Biological and Chemical Sensing, and Optically Based Materials for Defence, 599006 (October 15, 2005).

[8] David B. Joyce, Frederick Schmid. Progress in the growth of large scale Ti:sapphire crystals by the heat exchanger method (HEM) for petawatt class lasers. Journal of Crystal Growth 312 (2010) 1138–1141.

[9] A. A. Anderson, R. W. Eason, L. M. B. Hickey, M. Jelinek, C. Grivas, D. S. Gill, and N. A. Vainos, "Ti:sapphire planar waveguide laser grown by pulsed laser deposition," Optics Letters 22, 1556-1558 (1997).

[10] L. S. Wu, A. H. Wang, J. M. Wu, L. Wei, G. X. Zhu, and S. T. Ying, "Growth and Laser Properties of Ti-Sapphire Single-Crystal Fibers," Electronics Letters 31, 1151-1152 (1995).

[11] T. Fukada, P.Rudolph, S.Uda (Eds.).FiberCrystal Growth from the melt. Springer.August 2003.

[12] D.Sangla, N.Aubry, A.Nehari, A.Brenier, O.Tillement, K.Lebbou , F.Balembois,.Yb-doped Lu3Al5O12 fibers single crystals grown under stationary stable state for laser application. Journal of Crystal Growth 312(2009)125–130.

[13] H.S. Fang, Y.Y. Pan, L.L. Zheng, Q.J. Zhang, S. Wang, Z.L. Jin.To investigate interface shape and thermal stress during sapphire single crystal growth by the Cz method. Journal of Crystal Growth 363 (2013) 25–32.

[14] Chung-Wei Lu, Jyh-Chen Chen , Chien-Hung Chen (2010),. Effects of RF coil position on the transport processes during the stages of sapphire Czochralski crystal growth. Journal of Crystal Growth 312; 1074–1079.

[15] A. Nehari, T. Duffar, E.A. Ghezal, K. Lebbou. Cryst. Growth Des.2014, 14, 6492−6496.

[16] H. S. Fang, Z. W. Yan, and E. D. Bourret-Courchesne. Numerical Study of the Micro-Pulling-Down Process for Sapphire Fiber Crystal Growth. DOI: 10.1021/cg101021t .2011. CRYSTAL GROWTH &DESIGN Article. Vol. 11, 121 129.

[17] C.W. Lan, S. Uda, T. Fukuda. Theoretical analysis of the micro-pulling-down process for Gex Si1-xfiber crystal growth. Journal of Crystal Growth 193 (1998) 552Ð562. June 1998.

[18] A. Laidoune. Croissance des fibres cristallines pour usage dans l'optoélectronique. Thèse de doctorat. Université de Batna1,2010 Batna-Algeria.

[19] Abdeldjelil Nehari .Etude et caractérisation de la synthèse de milli-billes d'alumine alpha et de la cristallogenèse du saphir pur et dopé titane (Ti3+). THESE DE DOCTORAT L'UNIVERSITE DE LYON 2011.

[20] Gerd Wagner, Max Shiler, and Volker Wulfmeyer, Simulations of thermal lensing of aTi:Sapphire crystal end-pumped withhigh average power. OPTICS EXPRESS 8055, 3 October 2005 / Vol. 13, No. 20.